Catalysis Letters Vol. 88, Nos. 3–4, June 2003 (© 2003)

A comparison of catalytic oxidative dehydrogenation of ethane over mixed V-Mg oxides and over those prepared via a mesoporous V-Mg-O pathway

Zi-Sheng Chao and Eli Ruckenstein*

Department of Chemical Engineering, State University of New York at Buffalo, Amherst, NY 14260, USA

Received 5 February, 2003; accepted 28 March, 2003

The catalytic oxidative dehydrogenation of ethane was investigated in a fixed-bed tubular microreactor at 500, 550 and 600 °C and a space velocity of 35 027 ml g^{-1} h^{-1}. Two kinds of V-Mg oxides catalysts containing various V/Mg atomic ratios were employed. One group of catalysts was prepared by the solid reaction between fine powders of vanadium pentoxide and magnesium nitrate and the other ones were obtained from mesostructured V-Mg-Os. For the former catalysts, it was found that the selectivity to ethene increased and the conversion of ethane passed through a maximum with increasing V/Mg atomic ratio. For the catalysts obtained from the mesoporous materials, an optimum V/Mg atomic ratio was found, for which the conversion of ethane and the selectivity to ethene were maxima. Compared with the mixed-oxide catalysts, those obtained from the mesoporous materials exhibited much higher yields to ethene. Several new phases, such as *pyro*-$Mg_2V_2O_7$, *ortho*-$Mg_3(VO_4)_2$ and *meta*-MgV_2O_6, formed between magnesia and vanadia, were identified by XRD in the mixed V-Mg oxide catalysts; they may be responsible for the catalytic activity. In the catalysts prepared from mesoporous V-Mg-O, a V_2O_3 phase, which may contain highly dispersed magnesium, was identified and suggested to be responsible for the higher catalytic performance.

KEY WORDS: oxidative dehydrogenation; ethane; catalyst; mesoporous; vanadium; magnesium.

1. Introduction

There is an increasing interest in the conversion of the abundant light alkanes ($C_1 \sim C_4$) to more valuable light chemicals, such as olefins, oxygenates and aromatic hydrocarbons. Ethane is the second major component of the natural gas (3–20 mol%). The current commercial route for the conversion of ethane to ethene, which is a basic feedstock in the petrochemical industry, is the non-oxidative dehydrogenation of alkanes at high temperatures. However, this pathway has both chemical and technological limitations. The highly endothermic direct dehydrogenation reactions are favored by high temperatures, but require a large input of heat and are associated with the deposition of coke on the catalyst and reactor and the generation of lower molecular weight alkanes. The above drawbacks of the direct dehydrogenation route have stimulated the search for better solutions based on the oxidative dehydrogenation (ODH) of light alkanes. Since these reactions are carried out in the presence of O_2 or air, the large endothermic heat required for dehydrogenation is more than compensated by the higher exothermic heat resulting from the oxidation of H_2 (one of the dehydrogenation products). Consequently, the total reaction heat for the production of alkenes becomes exothermic. The consumption of H_2 in the reaction zone also shifts the equilibrium toward the formation of alkenes. Furthermore, the ODH can be performed at lower temperatures by a proper selection of a catalyst. However, some technical difficulties must be overcome before the ODH becomes commercially viable. For instance, the alkenes formed are much more reactive than the initial alkanes, and it is difficult to prevent their combustion to CO_x (CO and CO_2), and hence to carry out the dehydrogenation with high selectivities to alkenes. This issue is closely connected with the finding of a proper catalyst with high activity and selectivity and the control of the reaction heat generated. Until now, numerous catalysts were employed for the ODH of ethane, and several systems have exhibited high selectivities to ethene and large conversions of ethane. For example, Velle *et al.* [1] studied the ODH of ethane over the perovskite-type catalysts $SrCe_{1-x}Yb_xO_{3-0.5x}$ in the temperature range from 500 to 700 °C. Using $SrCe_{0.5}Yb_{0.5}O_{2.75}$ as catalyst, they obtained a maximum yield of ethene of 49% with a selectivity of 70% at 700 °C. Alkaline earth–rare earth oxides were also proven to be effective catalysts for the ODH of ethane at high temperatures. Choudhary *et al.* [2] reported ethane conversions of 20 and 68% with ethene selectivities of 75 and 82% at 700 and 850 °C, respectively. However, the authors of references [1] and [2] did not report results in the absence of a catalyst. A non-catalytic ODH that occurred in an empty reactor at 600 °C [3] provided a yield and a selectivity to ethene of

---

* To whom correspondence should be addressed.
E-mail: feaeliru@acsu.buffalo.edu

1011-372X/03/0600–0147/0 © 2003 Plenum Publishing Corporation

33.2 and 73.7%, respectively. Mullar *et al.* [4] recently studied the non-catalytic and catalytic ODH of ethane. They noted that above 700 °C the non-catalytic ODH reaction was dominant with ethene yields of 46 and 53% and selectivities of 66 and 65% at 750 and 800 °C, respectively. In the presence of a $SrLaNdO_x$ catalyst [4], they obtained an ethene yield of 46% with a selectivity of 71% at 700 °C. The alkali oxides or salts were reported to promote the ODH of ethane. An ethene yield of 48.2% with a selectivity of 89.2% at 620 °C over a La_2O_5–CaO catalyst promoted with Li_2O was obtained by Ji *et al.* [5]. Conway *et al.* [6] obtained over a Dy_2O_3/MgO catalyst promoted with LiCl an ethene yield of 62.9% with a selectivity of 81.3% at 570 °C. The alkali and/or Cl promoted bismuth-based catalysts, $PbBi_3O_4Cl_3$ and $KSr_2Bi_3O_4Cl_6$ [7], provided ethene yields of 45 and 41.7% with selectivities of 87.6 and 92.2% respectively at 620 °C. However, the stability of the promoted catalysts presented a problem because of the loss of alkali and/or Cl during reaction at high temperatures. Zhou *et al.* [8] and Chao *et al.* [9] developed a novel group of catalysts, MF_2–ReOF (M = Ca, Sr and Ba, Re = La, Ce, Sm, Y, Ho, Pr, Nd), for the ODH reaction. The catalysts were stable and could be operated at high space velocities in the absence of an inert diluting gas. Ethene yields above 45% with selectivities above 60% have been obtained in the temperature range of 480 to 660 °C. Thorsteinson *et al.* [10] reported a MoVNb catalyst over which a 34% yield of ethene with a selectivity of 68% was obtained at 400 °C. A hetero-homogeneous process for the ODH of ethane, which is autothermal because the heat produced by the exothermic oxidative reaction is used in the endothermic thermolysis, was also employed. A 55% ethene yield was recently reported over a $LaMnO_3$-based monolithic catalyst with a honeycomb morphology at 900 °C [11].

In contrast to the large number of papers regarding the ODH of ethane to ethene, much fewer were concerned with the conversion of ethane to oxygenate or aromatic compounds. Some examples are the catalytic partial oxidation of ethane to acetic acid over MoVM (M = Nb, Pd [10], Al, Ga, Bi, Sb and Te [12]) catalysts, to acetaldehyde over VPO [13] catalysts, to formaldehyde over BPO_4-based catalysts [14,15] and to BTX (benzene, toluene and xylene) over ZSM-5 or APO-5 based catalysts [16,17].

The mesoporous silicates, such as MCM-41 [18], possess unique properties such as large and uniform-sized pores, high specific surface areas and high thermal stabilities. They are expected to be useful in selective adsorption and catalysis [19–24], because they facilitate diffusion. Recently, Zhang *et al.* [25] studied the partial oxidation of lower alkanes over vanadium-containing MCM-41 catalysts and found that for the ODH of ethane, the conversion increased with increasing vanadium content. An ethane conversion of about 18% and an ethene selectivity of about 50% were obtained at 550 °C. Solsona [26] examined the ODH of alkanes over vanadium oxide supported on mesoporous MCM-41 catalysts, and observed that the selectivity to ethene increased but the conversion of ethane decreased with increasing V loading. An ethene yield of 10.8% with a selectivity of 38.3% was obtained over a 10 wt%-V/MCM-41 catalyst at 600 °C.

In our laboratory, mesostructured V-Mg-O materials have been synthesized [27,28] and, in the present paper, the catalytic ODH of ethane is carried out over catalysts prepared from mesoporous V-Mg-O. Their catalytic performance was compared with that of the mixed fine V-Mg oxide powders and an attempt is made to identify the active phases in these catalysts.

2. Experimental

2.1. Catalyst preparation

All reagents were purchased from Aldrich and used without further purification. Five mesostructured V-Mg-O catalysts were prepared using vanadium (III) acetylacetonate ($V(acac)_3$) as vanadium source and magnesium chloride ($MgCl_2 \cdot 6H_2O$) as magnesium source. The templates employed were cetyltrimethylammonium bromide (CTAB) alone or an equimolar mixture of CTAB and sodium dodecylbenzene sulfonate (SDBS). The preparation was carried out as follows. First, $MgCl_2 \cdot 6H_2O$ and the template were dissolved into an aqueous solution of hydrochloric acid with vigorous stirring at room temperature, and $V(acac)_3$ was separately dispersed homogeneously into distilled water with vigorous stirring at room temperature for about 2 h. Then, the solution containing vanadium was added slowly into that containing magnesium and the template, again with vigorous stirring, at room temperature. The pH of the mixture formed was adjusted to 10.0 with a dilute aqueous solution of NaOH and monitored with a Corning® Chekmite pH-10 pH-meter (Corning Inc.), with a resolution of 0.02. The final mixtures had the molar compositions of

$$a\,V(acac)_3 : b \quad MgCl_2 : \quad 0.25 \text{ Surfactant} : \ 295\ H_2O$$

where a/b was varied between 4 : 1 and 1 : 4 and $a + b = 2$. After stirring at room temperature for an additional 24 h, the mixture was allowed to age at room temperature for 2 days. The solid product was recovered by filtration, washed with distilled water and dried at 100 °C for 12 h. To remove the surfactant, the specimens were heated in a flow of argon from room temperature up to 750 °C at a heating rate of 10 °C min^{-1} and kept at 750 °C for 4 h. The catalytic experiments and the N_2 adsorption–desorption measurements have been carried out after the removal of the surfactant.

The mixed metal oxide V-Mg-O catalysts were prepared via solid-state reactions. Calculated amounts of V_2O_5 and $Mg(NO_3)_2 \cdot 6H_2O$ were mixed and ground thoroughly in a mortar, and the mixture of fine powders obtained was calcined at 700 °C for 2 h after heating from room temperature at a rate of $4\,^{\circ}C\,min^{-1}$.

2.2. *Catalyst characterization*

X-ray diffraction (XRD) powder analysis was performed on a SIEMENS D500 diffractometer with a Cu Kα radiation of 1.5406 Å. The diffraction data were recorded for 2θ angles ranging between 1 and 50°, with a resolution of 0.02°.

N_2 adsorption–desorption measurements were carried out at the liquid nitrogen temperature, using a Micromeritics ASAP 2010 Gas Sorption and Porosimetry instrument. The specimen was loaded in this apparatus for outgassing at 350 °C until a vacuum of 1×10^{-3} Torr was attained and kept under this vacuum for an additional 4 h. The specific surface area was determined by the BET method and the pore volume was calculated at a relative pressure of $P/P_0 > 0.99$, assuming full surface coverage with nitrogen. The pore size distribution was calculated, using the N_2 desorption branch, by the BJH (Barrett–Joyner–Halenda) method.

The chemical compositions of the catalysts were determined by Atomic Absorption Spectrophotometry, using a Perkin–Elmer model AAS 3030 spectrophotometer. The specimens were first calcined at 600 °C in air for 4 h to completely remove the organic surfactants and then digested in a mixed solution of nitric and muriatic acids in a LEM MOS2000 Microwave Digester. Magnesium was determined by the Acetylene/Air Flame Atomic Absorption Spectrophotometry at a wavelength of 285.2 nm, and vanadium by the Acetylene/Nitrous Oxide Flame Atomic Absorption Spectrophotometry at a wavelength of 318.4 nm.

2.3. *Catalytic performance evaluation*

The catalytic performance was determined at atmospheric pressure in a tubular fixed-bed quartz microreactor (internal diameter = 5 mm). The catalyst (0.2 g) was introduced on quartz wool in the middle of the reactor and the space above the catalyst bed was filled with quartz granules. The reactor was located in a tubular furnace with the catalyst bed held in the constant temperature zone. The temperature was determined with a thermocouple in contact with the external surface of the reactor in the region of the catalyst bed. A reactant mixture containing ethane, oxygen and nitrogen was passed through the reactor at a temperature between 500 and 600 °C and a space velocity of $35\,027\,ml\,g^{-1}\,h^{-1}$. The compositions of the reactant mixture and gaseous effluent from the reactor were analyzed on-line using an SRI 8610C gas chromatograph equipped with Thermal Conductivity Detector (TCD) and Flame Ionization Detector (FID). The components were separated at programmed temperatures and pressures on a Hayesep DB ($30' \times \frac{1}{8}''$) packed column and then allowed to flow into the TCD and FID detectors. The inorganic gaseous components (N_2, O_2, CO and CO_2) were identified with the TCD and the organic ones (C_1–C_3 hydrocarbons) with the FID, in order to attain a high resolution.

3. Results and discussion

Table 1, which summarizes the textural properties of the mixed V-Mg-O catalysts, shows that the surface areas and pore volumes of the pure V_2O_5 and MgO and of the mixed-oxide catalysts are small. The mixed-oxide catalysts with atomic ratios of $V/Mg > 1.0$ had lower specific surface areas and pore volumes than the pure V_2O_5. The specific surface areas and the pore volumes of the catalysts increased with decreasing V/Mg atomic ratio and for $V/Mg \leq 1.0$ became larger than those of the pure V_2O_5. In all cases, the specific surface area and the pore volume of the mixed-oxide catalysts were smaller than those of the pure MgO. The pore size distributions (not included here) were broad. The porosity of these materials is probably mainly due to the interparticle pores.

The reactivities over the mixed V-Mg oxide catalysts are presented in figure 1 and table 2. It was found experimentally that the ODH of ethane in the empty reactor had a very low reactivity under the conditions employed. No reaction occurred at temperatures $\leq 500\,^{\circ}C$. At 550 and 600 °C, ethane conversions of 0.62% and 1.39% with ethene selectivities of 39.14 and 71.85% were obtained, respectively. The pure magnesium oxide and vanadium oxide provided poor reactivities and no reaction occurred at temperatures lower than 550 °C.

Figure 1(a) shows that, in the catalytic reaction over the mixed oxides, the conversion of ethane passed through a maximum at a V/Mg atomic ratio of about

Table 1
Textural properties of mixed V-Mg-O catalysts with different V/Mg atomic ratios

Atomic ratio V/Mg	BET ($m^2\,g^{-1}$)	Pore volume ($cm^3\,g^{-1}$)	Average pore size (nm)
∞[a]	4.75	0.01	8.28
4	1.02	0.0028	10.83
2	2.19	0.0071	12.65
1	6.36	0.017	10.63
0.5	6.54	0.017	10.61
0.25	7.16	0.023	12.78
0[b]	14.10	0.043	12.20

[a,b] Refer to the pure V_2O_5 and the pure MgO, respectively.

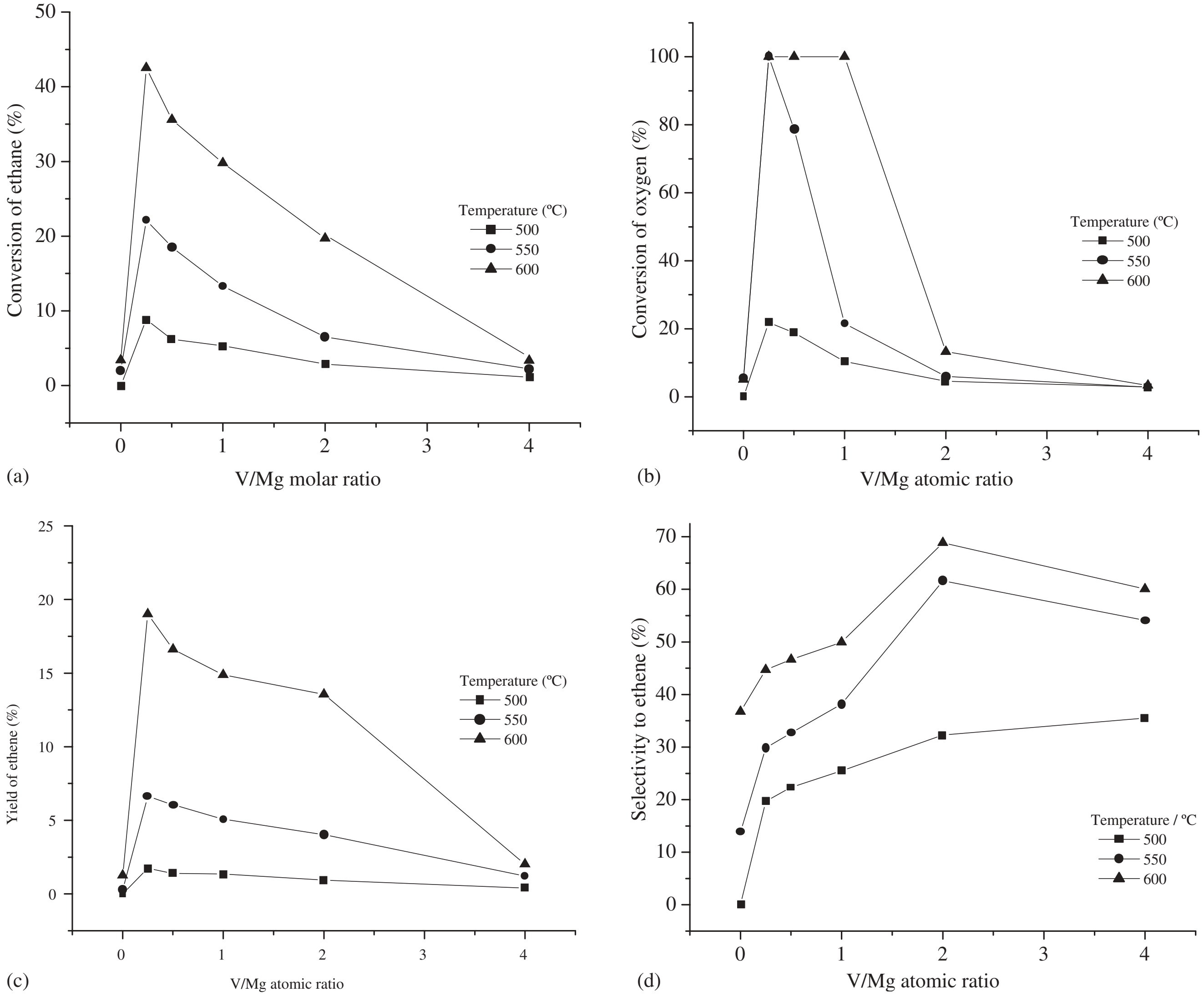

Figure 1. Reactivities of mixed V-Mg-O catalysts with different V/Mg atomic ratios.

0.25, after which it decreased with increasing V/Mg atomic ratio. This trend was stronger at higher temperatures. The conversion of O_2 (figure 1(b)) exhibited a stronger dependence on the V/Mg ratio and temperature. With increasing V/Mg atomic ratio, the conversion of O_2 passed through a maximum, after which it decreased slowly at 500 °C and more rapidly at 550 and 600 °C. A 100% conversion of O_2 could be achieved at 550 and 600 °C and low V/Mg ratios. The effect of the temperature and of the V/Mg atomic ratio on the yield of ethene was similar to that on ethane conversion (figure 1(c)). The selectivities are listed in table 2, which shows that those to C_2H_4 and CO_x (CO and CO_2) are much larger than those to CH_4 and C_{3+} (C_3H_6 and C_3H_8). For the same V/Mg atomic ratio, the selectivities to C_3H_8 and CO_x decreased with increasing temperature, while those to CH_4 and C_3H_6 increased, indicating that the higher temperatures favored the reactions involving the cleavage of the C–H and C–C bonds. At the same temperature, the selectivity to CO_x decreased and those to hydrocarbons (CH_4 and C_{3+}) increased with increasing V/Mg atomic ratio, indicating that a higher amount of magnesium stimulated the non-selective conversion of ethane. The selectivity to ethene appears to increase with increasing V/Mg ratio (figure 1(d)).

Table 3, which summarizes the textural properties of the mesostructured V-Mg-O catalysts, shows that with increasing V/Mg atomic ratio, the specific surface area of the catalyst slightly increased. The pore volumes and average pore sizes of these catalysts were in the ranges of 0.16–0.18 $cm^2\ g^{-1}$ and 3.99–4.66 nm, respectively. The pore size distributions (not included) of these catalysts were narrow, probably because they partially kept the order of the mesoporous structure. By comparing tables 1 and 3, one can see that the catalysts prepared from the mesoporous V-Mg-O had much larger specific surface areas and pore volumes but smaller average pore sizes.

The reactivities over these catalysts are presented in figure 2 and table 4. The effects of temperature and of

Table 2
Selectivities over the mixed V-Mg-O catalysts with different V/Mg atomic ratios

V/Mg atomic ratios	Molar ratio $N_2/O_2/C_2H_6$	Temperature (°C)	Selectivity (%)					
			CO	CO_2	CH_4	C_2H_4	C_3H_6	C_3H_8
∞[a]	90.19 : 3.91 : 5.90	500	0.00	0.00	0.00	0.00	0.00	0.00
	90.19 : 3.91 : 5.90	550	0.00	0.00	1.61	96.85	0.00	1.54
	90.19 : 3.91 : 5.90	600	0.00	0.00	3.14	96.72	0.14	0.00
4	88.69 : 3.90 : 7.41	500	0.00	44.37	4.67	35.5	0.77	14.69
	88.69 : 3.90 : 7.41	550	0.00	28.72	4.33	54.11	0.69	12.15
	88.69 : 3.90 : 7.41	600	0.00	24.6	4.54	60.05	0.87	9.94
2	89.23 : 4.43 : 6.34	500	0.00	53.84	3.08	32.3	0.74	10.04
	89.23 : 4.43 : 6.34	550	0.00	30.79	2.92	61.63	0.55	4.11
	89.23 : 4.43 : 6.34	600	10.1	14.19	4.58	68.84	0.62	1.67
1	89.04 : 4.32 : 6.64	500	42.54	25.22	1.71	25.45	0.31	4.77
	89.04 : 4.32 : 6.64	550	35.52	22.65	1.55	38.17	0.2	1.91
	89.04 : 4.32 : 6.64	600	32.45	8.42	7.24	49.93	1.03	0.93
0.5	89.60 : 4.00 : 6.40	500	36.01	34.42	1.62	22.38	0.59	4.98
	89.60 : 4.00 : 6.40	550	42.73	21.92	0.89	32.7	0.26	1.5
	89.60 : 4.00 : 6.40	600	33.21	12.3	6.01	46.67	0.62	1.36
0.25	89.76 : 3.66 : 6.58	500	47.01	29.16	0.97	19.69	0.39	2.78
	89.76 : 3.66 : 6.58	550	40.03	24.00	3.80	29.84	0.29	2.04
	89.76 : 3.66 : 6.58	600	33.45	12.62	6.79	44.71	1.24	1.19
0[b]	90.19 : 3.91 : 5.90	500	0.00	0.00	0.00	0.00	0.00	0.00
	90.19 : 3.91 : 5.90	550	0.00	85.32	0.74	13.86	0.08	0.00
	90.19 : 3.91 : 5.90	600	0.00	61.04	2.06	36.76	0.14	0.00

[a,b] Refer to the pure V_2O_5 and the pure MgO, respectively.

the V/Mg atomic ratio on the conversion of ethane are presented in figure 2(a), which shows that the conversion of ethane increased with increasing temperature and that it passed through a maximum with increasing V/Mg atomic ratio. The maximum conversion of ethane occurred at an atomic ratio of V/Mg of about 10. The effects of temperature and V/Mg atomic ratio on the conversion of O_2 are presented in figure 2(b). At 550 and 600 °C, the conversion was much higher than that at 500 °C and passed through a maximum with increasing V/Mg atomic ratio. The dependence of the yield of ethene on the atomic ratio of V/Mg and temperature is similar to that for the conversion of ethane and is presented in figure 2(c). The selectivity to ethene passed through a maximum with increasing V/Mg atomic ratio (figure 2(d)). Table 4 lists the selectivities to the components in the gaseous effluent from the reactor. One can see that with the increase in temperature, the selectivities to CO, CH_4, C_3H_6 and C_2H_4 increased, while those to CO_2 and C_3H_8 decreased. With increasing V/Mg atomic ratio, the selectivity to ethene increased but to all other components decreased. By comparing figures 1 and 2, one can easily conclude that the mesoporous V-Mg-O-based catalysts provided higher yields and selectivities to ethene, but a smaller conversion of O_2.

Table 3
Textural properties of the catalysts based on mesoporous V-Mg-O with different V/Mg atomic ratios

Atomic ratio V/Mg	BET $(m^2 g-1)$	Pore volume $(cm^3 g^{-1})$	Average pore size (nm)
1.4	NA[a]	NA	NA
3.2	158.5	0.16	3.99
10.6	159.1	0.16	4.05
35.3	155.1	0.18	4.66
48.2	151.0	0.17	4.51

[a] Not available.

The XRD spectra of the mixed V-Mg-O catalysts are presented in figure 3. Compared to pure MgO (figure 3(a)) and V_2O_5 (figure 3(g)), several new phases were formed in the mixed V-Mg-O catalysts during their calcination (figure 3(b–f)). Over the catalyst with an atomic ratio V/Mg = 4 (figure 3(f)), two phases, V_2O_5 and *meta*-MgV_2O_6, could be identified. When the atomic ratio of V/Mg decreased to 2.0 (figure 3(e)), the intensities of the diffraction peaks specific for the V_2O_5 phase decreased but those for the MgV_2O_6 increased. When the atomic ratio of V/Mg was further decreased to 1 and 0.5, *pyro*-$Mg_2V_2O_7$ and MgO phases could be identified, besides the *meta*-MgV_2O_6 phase (figures 3(c) and (d)). For atomic ratios of V/Mg below 0.5, the phases *pyro*-$Mg_2V_2O_7$, *meta*-MgV_2O_6 and MgO as well as an additional phase, *ortho*-$Mg_3(VO_4)_2$, could be identified (figure 3(b)). No separated V_2O_5 phase could

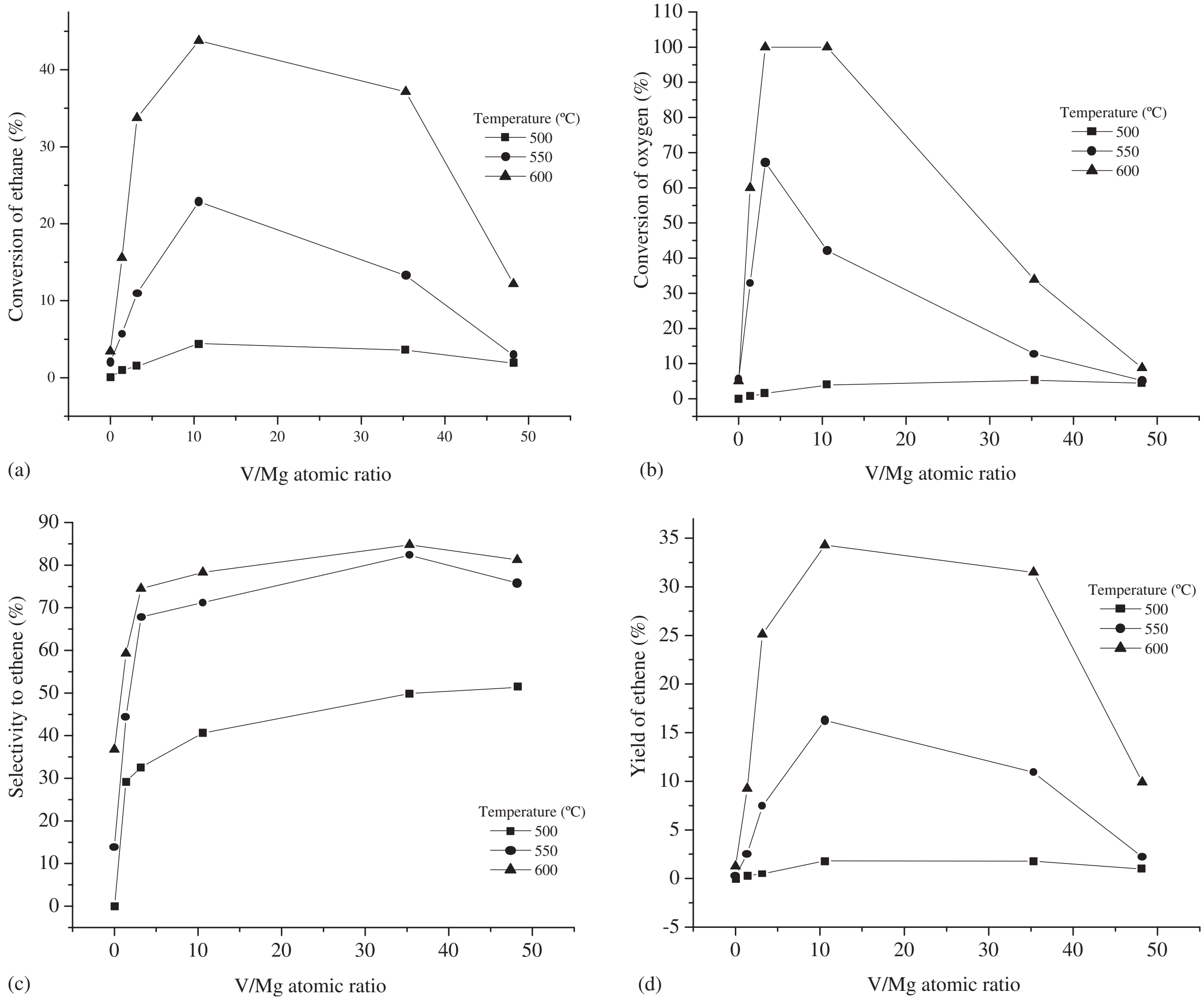

Figure 2. Reactivities of catalysts prepared from mesoporous V-Mg-O with different V/Mg ratios.

be identified in the catalysts with atomic ratios V/Mg < 2 and no separated MgO phase for atomic ratios V/Mg > 1.

The V-Mg-O catalysts were usually considered among the most active and selective catalysts in the ODH of short-chain alkanes ($C_3 \sim C_4$) to the corresponding alkenes [29–40]. They were prepared either by the impregnation of a magnesium-based support (*e.g.*, MgO, $Mg(OH)_2$) with a vanadium precursor solution, followed by calcinations at elevated temperatures, or by the solid-state reaction between fine magnesium and vanadium oxide powders. The nature of the active phases in the V-Mg-O catalysts was studied by many authors, but no final conclusion was yet reached. For example, Chaar *et al.* [29] suggested that the active phase is $Mg_3(VO_4)_2$, while Sam *et al.* [30] proposed that $Mg_2V_2O_7$ is the most selective phase in the ODH of propane. Corma *et al.* [32] and Gao *et al.* [33] suggested that the cooperation between both of the above phases affected the reactivity. Of course, only the surface compounds should be responsible for the catalytic behavior. These surface compounds can comprise those of the bulk, and possibly other ones, which are not present there.

In the range of low magnesium content, V_2O_5 may have acted as a support over which magnesium was highly dispersed, and a compound with a low magnesium content, such as the *meta*-MgV_2O_6, was formed. In contrast, in the range of high magnesium content, MgO may have played the role of the support over which vanadium was highly dispersed, and compounds with high magnesium contents, such as the *pyro*-$Mg_2V_2O_7$ and *ortho*-$Mg_3(VO_4)_2$), were formed. Because much higher performances for the ODH of ethane have been obtained over the mixed V-Mg-O catalysts than that over the pure magnesia and pure vanadia and the specific surface areas of the catalysts were not larger than that of MgO (see table 1), it is clear that the active phases were generated during the catalyst preparation. Furthermore, higher selectivities were obtained over the catalysts with higher vanadium content, but higher

Table 4
Selectivities over the catalysts based on mesoporous V-Mg-O with different V/Mg atomic ratios

V/Mg Atomic ratios	Molar ratio $N_2/O_2/C_2H_6$	Temperature (°C)	Selectivity (%)					
			CO	CO_2	CH_4	C_2H_4	C_3H_6	C_3H_8
1.4	88.79 : 4.39 : 6.82	500	0	56.48	3.05	29.21	1.34	9.92
	88.79 : 4.39 : 6.82	550	0	48.04	3.4	44.43	0.62	3.51
	88.79 : 4.39 : 6.82	600	8.32	26.01	4.31	59.31	0.56	1.49
3.2	88.36 : 4.71 : 6.93	500	0	50.04	4.44	32.6	1.32	11.6
	88.36 : 4.71 : 6.93	550	9.38	14.26	5.94	67.84	0.83	1.75
	88.36 : 4.71 : 6.93	600	12.51	3.26	6.87	74.46	1.5	1.4
10.6	88.74 : 4.5 : 6.76	500	0	45.05	3.7	40.62	0.56	10.07
	88.74 : 4.5 : 6.76	550	2.31	19.78	4.51	71.23	0.18	1.99
	88.74 : 4.5 : 6.76	600	7.3	2.66	7.95	78.29	1.61	2.19
35.3	89.71 : 3.97 : 6.32	500	0	38.48	3.08	49.85	0.22	8.37
	89.71 : 3.97 : 6.32	550	0	8.43	5.00	82.32	0.03	4.22
	89.71 : 3.97 : 6.32	600	2.01	2	7.29	84.77	1.54	2.39
48.2	88.77 : 4.38 : 6.84	500	0	32.62	3.43	51.37	0.97	11.61
	88.77 : 4.38 : 6.84	550	0	14.45	2.73	75.8	0.64	6.38
	88.77 : 4.38 : 6.84	600	0	10.77	5.33	81.21	0.68	2.01

conversion over those with higher magnesium content. Thus, the *pyro*-$Mg_2V_2O_7$ and *ortho*-$Mg_3(VO_4)_2$ might have been the most active phases and the *meta*-MgV_2O_6 the most selective one in the ODH of ethane.

The XRD spectra of the mesoporous V-Mg-O, after their heating at 750 °C, are presented in figure 4. In a wide range of V/Mg atomic ratios (10–48), only a V_2O_3 phase could be identified. A $Mg_{1.5}VO_4$ phase as well as the MgO phase could be additionally identified in the catalysts with V/Mg ratios smaller than 3.2. This may mean that in the former cases magnesium was highly dispersed over the large surface of V_2O_3 (see table 3) and could not be detected by XRD. Since high catalytic performances were achieved over the catalysts with atomic ratios of V/Mg of about 10, it is reasonable to consider that V_2O_3 promoted by highly dispersed magnesium was the active phase.

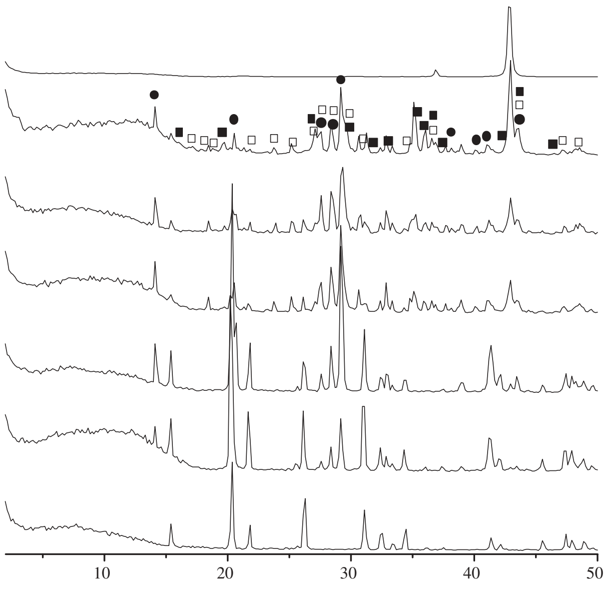

Figure 3. XRD spectra of mixed V-Mg-O catalysts with V/Mg atomic ratios of a: 0 (pure MgO); b: 0.25; c: 0.5; d: 1; e: 2.0; f: 4.0 and g: ∞ (pure V_2O_5). Symbols: (●) *meta*-MgV_2O_6; (■) *pyro*-$Mg_2V_2O_7$; (□) *ortho*-$Mg_3(VO_4)_2$. The intensities of the peaks for MgO were reduced by a factor of 10 to be able to present several spectra in a single figure.

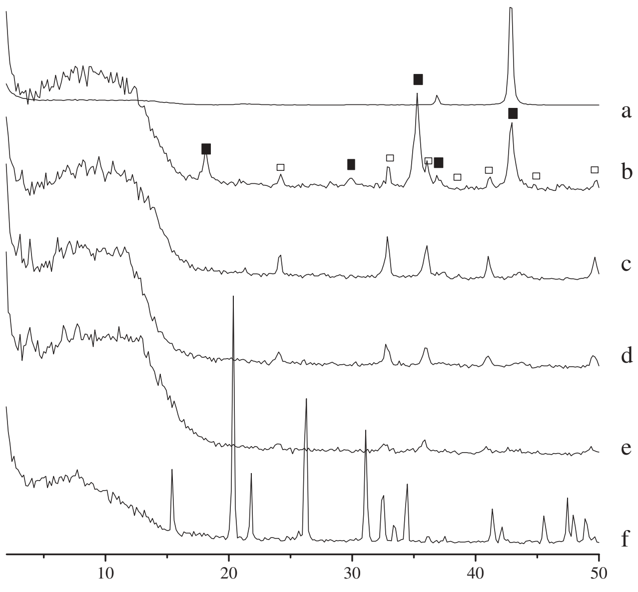

Figure 4. XRD spectra of catalysts prepared from mesoporous V-Mg-O with V/Mg molar ratios of a: 0 (pure MgO); b: 3.2; c: 10.6 d: 35.3; e: 48.2 and f: ∞ (pure V_2O_5) Symbols: (■) V_2O_3 and (□) $Mg_{1.5}VO_4$. The intensities of the peaks for MgO were reduced by a factor of 10 to be able to present several spectra in a single figure.

4. Conclusion

The V-Mg-O catalysts originated from mesoporous materials are more active and selective than the mixed V-Mg oxide ones in the catalytic ODH of ethane to ethene. The atomic ratio of V/Mg affected in both cases the phase compositions and catalytic performances.

References

[1] O.J. Velle, A. Anderson and K.J. Jens, Catal. Today 6 (1990) 567.
[2] V.R. Choudhary, B.S. Uphade and S.A.R. Mullar, Angew. Chem., Int. Ed. Engl. 34 (1995) 665.
[3] R. Burch and E.M. Crabb, Appl. Catal. 97 (1993) 49.
[4] S.A.R. Mullar, O.V. Buyevskaya and M. Baerns, Appl. Catal. A 226 (2002) 73.
[5] L. Ji and J. Liu, Chem. Commun. (1996) 1203.
[6] S.J. Conway, D.J. Wang and J.H. Lunsford, Appl. Catal. 79 (1991) L1.
[7] W. Ueda, S.W. Lin and I. Tohmoto, Catal. Lett. 44 (1997) 241.
[8] X.P Zhou, Z.S. Chao, H.L. Wan and K.R. Tsai, Appl. Catal. A 133 (1995) 263.
[9] Z.S. Chao, X.P Zhou, H.L. Wan and K.R. Tsai, China Patent ZL 94 1 17229 5, B01J 27/12.
[10] E.M. Thorsteinson, T.P. Wilson, F.G. Young and P.H. Kasai, J. Catal. 52 (1978) 116.
[11] F. Donsi, R. Pirone and G. Russo, J. Catal. 209 (2002) 51.
[12] W. Ueda and K. Oshihara, Appl. Catal. A 200 (2000) 135.
[13] L. Tessier, E. Bordes and M.G. Bonneau, Catal. Today 24 (1995) 335.
[14] Y. Uragami and K. Otsuka, J. Chem. Soc., Faraday Trans. 88 (1992) 3605.
[15] N.U. Zhanpeison and K. Otsuka, React. Kinet. Catal. Lett. 52 (1994) 27.
[16] A. Hagen, O.P. Keipert and F. Roessner, in 11th International Congress on Catalysis, J.W. Hightower, W.N. Delgass, E. Iglesia and A.T. Bell (eds); Stud. Surf. Sci. Catal. 101 (1996) 781.
[17] P. Concepcion, J.M.L. Nieto, A, Mifsud and J.P. Pariente, Appl. Catal. A 151 (1997) 373.
[18] J.S. Beck, J.C. Vartuli, W.J. Roth, M.E. Leonowicz, C.T. Kresge, K.D. Schmitt, C.T.W. Chu, D.H. Olson, E.W. Sheppard, S.B. McCullen, J.B. Higgins and J.L. Schlenker, J. Am. Chem. Soc. 114 (1992) 10834.
[19] P. Behrens, Adv. Mater. 5 (1993) 127.
[20] A. Sayari, Chem. Mater. 8 (1996) 1840.
[21] A. Corma, Chem. Rev. 97 (1997) 2373.
[22] D. Brunel, Micropor. Mesopor. Mater. 27 (1999) 329.
[23] J.Y. Ying, C.P. Mehnert and M.D. Wong, Angew. Chem., Int. Ed. Engl. 38 (1999) 56.
[24] P. Selvam, S.K. Bhatia and C.G. Sonwane, Ind. Eng. Chem. Res. 40 (2001) 3237.
[25] Q. Zhang, Y. Wang, Y. Ohishi, T. Shishido and K. Takehira, J. Catal. 202 (2002) 308.
[26] B. Solsona, T. Blasco, J.M. Lopez Nieto, M.L. Pena, F. Rey and A. Vidal-Moya, J. Catal. 203 (2002) 443.
[27] Z.S. Chao and E. Ruckenstein, Langmuir 18 (2002) 734.
[28] Z.S. Chao and E. Ruckenstein, Chem. Mater. 14 (2002) 4611.
[29] M.A. Chaar, D. Patel and H.H. Kung, J. Catal. 109 (1988) 463.
[30] D.S.H. Sam, V. Soenem and J.C. Volts, J. Catal. 123 (1990) 417.
[31] P.M. Michalkos, M.N. Kung, I. Jahan and H.H. Kung, J. Catal. 140 (1993) 226.
[32] A. Corma, J.M.L. Nieto and N. Paredes, J. Catal. 144 (1993) 425.
[33] X. Gao, P. Ruiz, Q. Xin, X. Guo and B. Delmon, J. Catal. 148 (1994) 56.
[34] S.R.G.C. Peres, J.P. Bernard, M. Ruwet, P. Ruiz and B. Delmon, J. Catal. 158 (1996) 452.
[35] A. Pantazidis, A. Auroux, J.M. Herrmann and C. Mirodatos, Catal. Today 32 (1996) 81.
[36] D.L. Stern, J.N. Michaels, L. Decaul and R.K. Grasselli, Appl. Catal. A 153 (1997) 21.
[37] H.H. Kung and M.C. Kung, Appl. Catal. A 157 (1997) 105.
[38] J.M.L Nieto, A. Dejoz, M.I. Vasquez, W.O. Leary and J. Cunningham, Catal. Today 40 (1998) 215.
[39] J.M.L Nieto, J. Soler, P. Concepcion, J. Herguido, M. Menedez and J. Santamaria, J. Catal. 185 (1999) 324.
[40] R.X. Valenzuela and V.C. Corberan, Top. Catal. 11 (2000) 153.